Computation of Laminar Hypersonic Compression-Corner Flows

David H. Rudy,* James L. Thomas,† Ajay Kumar,‡ and Peter A. Gnoffo§
NASA Langley Research Center, Hampton, Virginia 23665
and
Sukumar R. Chakravarthy¶
Rockwell International Science Center, Thousand Oaks, California 91360

A code validation study has been conducted using four different codes for solving the compressible Navier-Stokes equations. Computations for a series of nominally two-dimensional high-speed laminar separated flows were compared with detailed experimental shock-tunnel results. The shock-wave boundary-layer interactions considered were induced by a compression ramp. In general, good agreement was reached between two-dimensional grid-refined calculations and experiment for the incipient- and small-separation conditions. For the highly separated flow case, three-dimensional calculations, which included the finite-span effects of the experiment, were required in order to obtain agreement with the data. The finite-span effects were important in determining the extent of streamwise separation as well as the time required to establish the steady-flow interaction. The results presented provide a resolution of discrepancies with the experimental data encountered in several recent computational studies.

Nomenclature

C_f = skin-friction coefficient, $2\tau_w/\rho_\infty u_\infty^2$
C_h = heat transfer coefficient, $\dot{q}/\rho_\infty u_\infty(H_\infty - H_w)$
C_p = pressure coefficient, $2p/\rho_\infty u_\infty^2$
H = total enthalpy
L = reference length
M = Mach number
p = pressure
$\dot{q}$ = heat transfer rate
Re = unit Reynolds number, $\rho_\infty u_\infty/\mu_\infty$
T = temperature
u = streamwise velocity
x = streamwise coordinate
α = angle of attack
γ = ratio of specific heats
θ = compression-ramp angle
μ = molecular viscosity
ρ = density
τ = shear stress

Subscripts

a = reattachment point
s = separation point
w = wall
∞ = freestream

Presented as Paper 89-1838 at the AIAA 20th Fluid Dynamics, Plasma Dynamics and Lasers Conference, Buffalo, NY, June 12–14, 1989. Received Aug. 16, 1990; revision received Nov. 28, 1990; accepted for publication Dec. 3, 1990.

*Research Scientist, Computational Aerodynamics Branch. Member AIAA.
†Research Scientist, Computational Aerodynamics Branch. Associate Fellow AIAA.
‡Head, Theoretical Flow Physics Branch. Associate Fellow AIAA.
§Research Engineer, Aerothermodynamics Branch. Senior Member AIAA.
¶Head, Computational Fluid Dynamics Department. Member AIAA.

Introduction

THE need for development and validation of computational methods for solving the Navier-Stokes equations for high-speed flows has increased because of the National Aero-Space Plane project. The propulsion system of advanced hypersonic vehicles will likely use the external vehicle contours as compression and expansion surfaces for the inlet and nozzle, respectively. Thus, the integration of the engine and airframe is an important design consideration. This design process relies heavily on the development of computer codes with appropriate geometric flexibility and physical models since many of the high Mach number, high-enthalpy flow conditions the vehicle may encounter in flight cannot presently be simulated in ground-based facilities.

Before such a code can be used with confidence as an analysis or design tool, the range of validity of the solution procedure and physical modeling must be known. The verification process typically involves three distinct types of testing: 1) internal consistency checks, 2) comparisons with other codes, and 3) comparisons with experimental data. The first of these tests consists of checking the code for proper conservation of mass, momentum, and energy. For instance, the simplest test would be verifying that the code can preserve freestream flow. Other tests would include the computation of flows for which analytic solutions are available. In these tests, studies can be made of the effects of grid refinement and parameter variations in the numerical scheme. The second level of testing is the comparison of computed results with those obtained using other similar but well-established codes that also solve the Navier-Stokes equations. Comparisons could also be made with results from boundary-layer codes or space-marching parabolized Navier-Stokes codes for appropriate test problems. The third level of testing is the comparison of computed results with highly accurate benchmark experimental data sets.

The present paper describes a comparison of computed results from four different computer codes for solving the compressible Navier-Stokes equations with experimental data. The test problem considered has features typical of high-speed internal flow problems of practical importance in the design and analysis of the inlet portion of a scramjet engine on an advanced hypersonic vehicle. Previous related code-validation studies are given by Rudy et al.[1] and Thomas et al.[2]

Description of Codes

CFL3D

Three of the four computer codes use similar recently developed upwind technology. The first of these, CFL3D (Computational Fluids Laboratory three-dimensional code), was developed by Thomas for the thin-layer Navier-Stokes equations and is described in Ref. 3. This code uses a finite-volume method in which the convective and pressure terms are discretized with the upwind-biased flux-difference splitting technique of Roe. The reconstruction of the cell-centered variables to the cell-interface locations is done using a monotone interpolation of the primitive variables such that third-order accuracy in one-dimensional inviscid flow is obtained. The differencing for the diffusion terms representing shear stress and heat transfer effects corresponds to second-order-accurate central differencing so that the global spatial accuracy of the method is second order. The time-differencing algorithm is a spatially-split approximate-factorization scheme.

USA-PG2

The second of the upwind codes, USA-PG2 (Unified Solution Algorithm-Perfect Gas, two-dimensional), was developed by Chakravarthy[4] and solves the full Navier-Stokes equations. The corresponding three-dimensional version is designated USA-PG3. In these codes, the convective terms are modeled using a family of high-accuracy total-variation-diminishing (TVD) upwind-biased finite-volume schemes based on Roe's approximate Riemann solver. Second-derivative viscous terms, except cross-derivative terms, are modeled with conventional central-difference approximations. The cross-derivative terms are treated so that their discretization also contributes to the diagonal dominance of the implicit time discretization. For the present calculations, the implicit formulation was solved using approximate-factorization methods.

LAURA

The third upwind code, LAURA (Langley Aerothermodynamic Upwind Relaxation Algorithm), is a finite-volume, single-level storage implicit upwind-differencing algorithm developed by Gnoffo[5,6] to solve the full and thin-layer Navier-Stokes equations with particular emphasis on external, reacting, hypersonic flows over blunt bodies with detached shock waves. The perfect-gas version was implemented in the present study. The inviscid components of flux across cell walls are described with Roe's averaging and Harten's entropy fix with second-order corrections based on Yee's Symmetric TVD scheme. The viscous terms are discretized using central differences. A point-implicit relaxation strategy is used.

NASCRIN

The fourth computer code NASCRIN (Numerical Analysis of Scramjet Inlets), was developed by Kumar[7,8] and uses the original unsplit explicit technique of MacCormack[9] to solve the full Navier-Stokes equations. This technique is a two-step, predictor-corrector scheme that is second-order accurate in both space and time. Fourth-order artificial viscosity based on the gradients of pressure and temperature is used near shock waves to suppress numerical oscillations.

Test Case

The test case considered in the present study is shown schematically in Fig. 1. This case, which has viscous/inviscid interactions typical of those found in the flowfield within the propulsion system of a hypersonic vehicle, is the two-dimensional flow over a compression corner formed by the intersection of a flat plate and a wedge tested by Holden and Moselle[10] in the Calspan 48-in. shock tunnel. The flowfield shown in Fig. 1 shows the separated flow that forms in the corner region for a sufficiently large wedge angle. Downstream of the reattachment point, the boundary layer thins

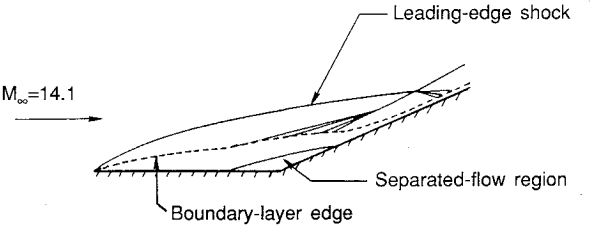

Fig. 1 Test case: compression corner.

rapidly due to the compression, resulting in large increases in skin friction and heat transfer on the wedge surface. Furthermore, the compression waves produced by the corner coalesce into a shock wave that intersects with the leading-edge shock, producing an expansion fan and a shear layer, both of which affect the flow on the ramp. Three wedge angles tested by Holden and Moselle[10] are considered here. The flow remained attached on the 15-deg wedge, a small separated-flow region occurred with the 18-deg wedge, and a large separated-flow region was produced by the 24-deg wedge.

The nominal flow conditions for this case were $M_\infty = 14.1$, $T_\infty = 160°\text{R}$, and $Re = 7.2 \times 10^4/\text{ft}$. The wall temperature T_w was 535°R. The Reynolds number was low enough that the flow remained completely laminar, thereby eliminating the issue of turbulence modeling from the present study. Furthermore, even though the freestream Mach number was high, the freestream temperature was low enough that there were no significant real-gas effects. In the experiment, values of surface pressure, skin friction, and heat transfer were measured in the center plane of the model, which had a spanwise length that was thought to be sufficient to produce two-dimensional flow in the measurement region.

This test case has been used in previous computational studies by other investigators. The first computation using the full Navier-Stokes equations for this case was made by Hung and MacCormack.[11] They obtained good agreement with the experimental data for the 15- and 18-deg wedges, but their solution significantly underpredicted the size of the separated-flow region for the 24-deg wedge. Recent studies have been presented by the Power and Barber,[12] Ng et al.,[13] and Rizzetta and Mach.[14] In addition, the fully attached flow with the 15-deg wedge has been used for comparisons with computations using the parabolized Navier-Stokes equations in various studies such as in Refs. 15–17.

Results and Discussion

Compression-Corner Case

Comparisons were made between the computed solutions from all four codes and experimental data for the 15- and 24-deg wedges using two different grids. The first grid had 51 points in the streamwise direction and 51 points in the vertical direction. In the streamwise direction, the grid was clustered near the leading edge of the flat plate and in the corner region. In the normal direction, the grid was clustered near the model surface. Above the wedge, a simple sheared grid was used, producing a nonorthogonal grid in this region. A second grid with twice the resolution was constructed from the first grid using 101 points in each direction while maintaining the same grid stretching.

15-Degree Wedge

Figure 2a shows a comparison of the computed surface-pressure coefficient with experimental values for all four codes on two different grids. The pressure coefficient is plotted as a function of x/L, where x is measured from the leading edge of the flat plate and L is the length of the flat plate portion of the model. As shown, there are only very slight differences in the predictions from the four codes for the 51 × 51 grid; however, the four solutions are virtually identical for the 101 × 101 grid. The computed pressures are generally higher

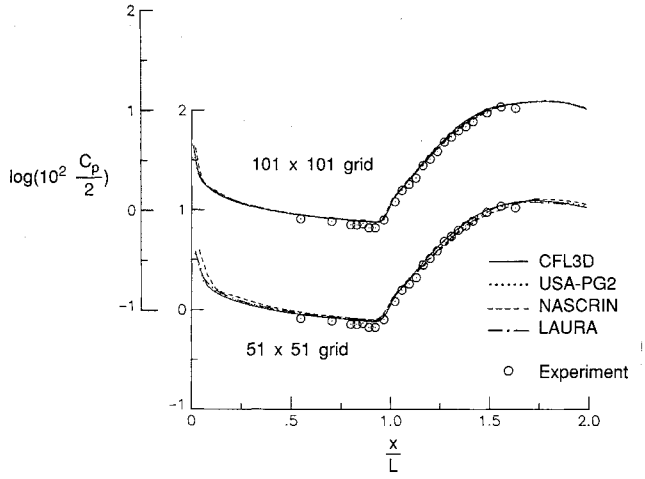

a) Surface pressure

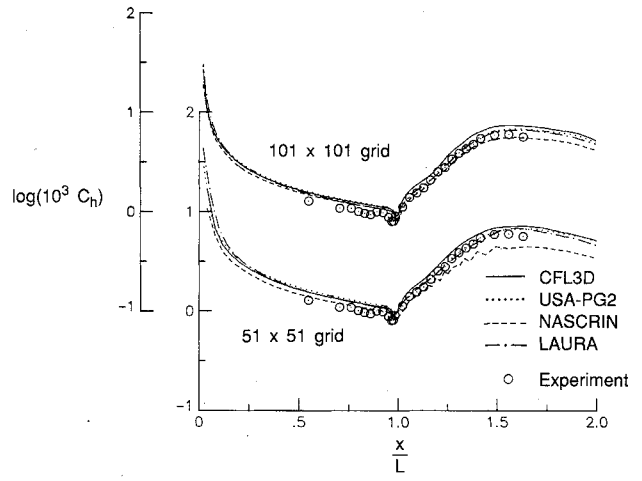

b) Surface heat transfer

Fig. 2 Comparison of computation and experiment for 15-deg wedge.

than the experimental values even on the flat plate portion of the model. However, the computed pressures were in excellent agreement with those given by hypersonic strong-interaction theory (not shown). The corresponding comparison of the computed surface heat transfer coefficient with experimental values for all four codes on the two grids is shown in Fig. 2b. As with the pressure coefficient, the calculations on the 101 × 101 grid produce the best agreement among the codes. The largest differences occur along the ramp. The trends in the experimental data are again predicted well, but the computed values are generally slightly higher than those found in the experiment.

It should be noted that all of the plots shown in the present paper for the compression-corner case differ from those given in Ref. 18 in two ways. First of all, the experimental data have been revised by Holden, who recomputed the freestream conditions using the tunnel calibration rather than using pitot-tube measurements from probes within the shock layer emanating from the leading edge. The resulting change in the surface coefficient data eliminated the need for the 1-deg angle-of-attack correction, which was necessary in Ref. 18 to match the experimental values of pressure on the flat plate portion of the model. Second, the data were originally given in Ref. 10 as a function of the distance along the surface of the model but were interpreted as being a function of the streamwise distance x in the plots in Ref. 18. Thus, the data on the ramp in Ref. 18 were shifted slightly downstream from their correct location.

24-Degree Wedge

Figure 3 shows the streamlines of the flowfield of the 24-deg wedge computed using the USA-PG2 code. The large size of the separated-flow region and the thinning of the boundary layer on the ramp downstream of the reattachment point can be clearly seen. Figure 4 shows the comparison of the computed surface-pressure coefficient with experimental values for this case. The four codes predict different extents of separation even with the 101 × 101 grid. A solution using a 201 × 201 grid was also made CFL3D. The predictions for surface pressure, skin friction, and surface heat transfer for this grid were almost identical to those found with the 101 × 101 grid with only a slight increase in the predicted extent of separation. Therefore, the 101 × 101 grid calculation with CFL3D can be considered to be sufficiently grid-refined for this flow. All four of the codes demonstrated a trend with grid convergence toward a similar longitudinal extent of separation that is much larger than that found in the experiment. As a result of the larger separation extent, the shock interaction is altered, moving the peak value of pressure on the ramp downstream in comparison to the experiment.

Time-Accurate Computations

In order to help resolve these differences between the computation and experiment, time-accurate calculations were made with three of the codes to study the question of whether the experimental data might have been obtained before steady flow had been fully established during the short run time available in the shock tunnel. The flow in the experiment reached a steady state in approximately 4 ms, and the total run time was approximately 10 ms. Figure 5 shows the solutions obtained with CFL3D at five intermediate times 1 ms apart between 1 and 5 ms. These results are representative of the time variation computed with all three of the codes used, CFL3D, USA-PG2, and NASCRIN. It can be seen that the separated-flow region is predicted reasonably well at a point in time between 2 and 3 ms, but the size of the region

Fig. 3 Streamlines for flow past 24-deg compression corner, USA-PG2 solution.

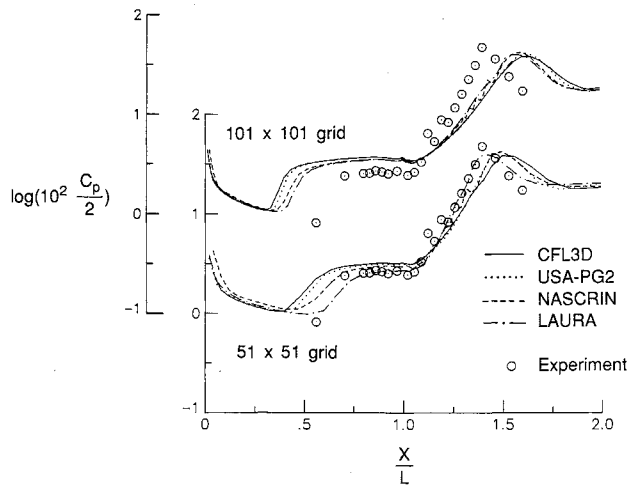

Fig. 4 Comparison of computation and experiment for 24-deg wedge.

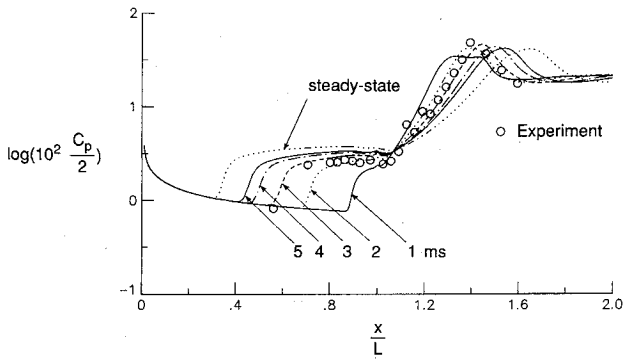

Fig. 5 Time history of surface pressure, CFL3D solution, 24-deg wedge.

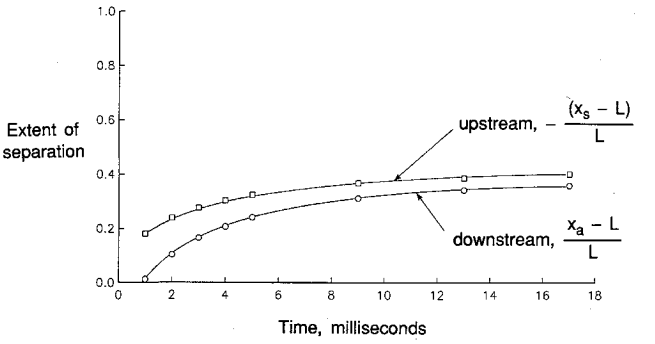

Fig. 7 Time history of separation extent for 21-deg wedge, CFL3D solution.

continues to increase as the solution is further advanced in time. It took more than 12 ms to establish steady flow in the computations, which is considerably longer than the testing time available in the experiment.

Calculations were also made with CFL3D for wedge angles of 18, 19.5, 21, and 22.5 deg. (Calculations made with USA-PG2 for 18- and 21-deg wedges verified the CFL3D results.) The results of these computations are summarized in Fig. 6, which shows the effect of wedge angle on the size of the separated-flow region. For the smallest separated-flow region, which occurred with the 18-deg wedge, the extent of separation using a 101 × 101 grid underpredicted the experimental value by approximately 23%. For the 24-deg wedge, the computed extent of separation overpredicted the experimental value by approximately 48% for the 101 × 101 grid. The 21-deg wedge case produced a computed separated-flow region comparable in size to that found experimentally with the 24-deg wedge. Figure 7 shows the positions of the upstream and downstream boundaries of the separated-flow region for this case as functions of time. As shown, it required significantly more time than 4 ms for the computed flowfield to reach its steady state even for a separated-flow region with a size comparable to that found in the experiments.

Three-Dimensional Calculations

Since the results from the two-dimensional computations did not match the experimental data, three-dimensional calculations were made with CFL3D to investigate the possibility of flow in the spanwise direction affecting the flow in the center of the plate. For the experimental data for which comparisons are shown later, no side plates were used. The spanwise length of the plate was 2 ft. Calculations were made with two different grids. One grid had 51 points in the streamwise direction, 51 points in the normal direction, and 25 points in the spanwise direction. The second grid had 101 points each in the streamwise and normal directions and 25 in the spanwise direction. In each case, the spanwise grid contained 19 points on the plate and 6 points in the freestream. Since the flow is symmetric about the center plane, the computational domain included only half of the plate. Approximate supersonic outflow boundary conditions were used at the sides of the computational domain outside of the ramp surface. Figure 8 shows results from the calculation with a 101 × 101 grid in each streamwise plane. The streamlines in the flow very near the model surface are visualized using particle traces. The separation and reattachment lines show that the size of the separated-flow region decreases across the plate from the center plane to the edge. The pressure contours in the downstream plane on the ramp at the end of the computational domain show an expansion of the flow in the spanwise direction near the edge of the plate to reduce the pressure to the freestream value. A comparison of the computed two- and three-dimensional center plane surface-pressure distributions with the experimental data is shown in Fig. 9 using solutions from CFL3D for all of the grids used in the present study. As shown, the three-dimensional effects produce a smaller separated-flow region in the center plane than that predicted in the two-dimensional calculations. Furthermore, the size of the separated-flow region and the pressure level in that region are in excellent agreement with the data for the finest mesh in the three-dimensional calculation. In addition, the computed pressure rise on the surface of the wedge is well predicted.

Figure 10 shows the normalized locations relative to the start of the compression ramp of the upstream and downstream boundaries of the separated-flow region as functions of time for both the two- and three-dimensional computations with CFL3D for the 24-deg wedge. Quite surprisingly, the time to establish the steady state for the three-dimensional flow is dramatically less than that required for the two-dimensional flow. For the three-dimensional computation, a

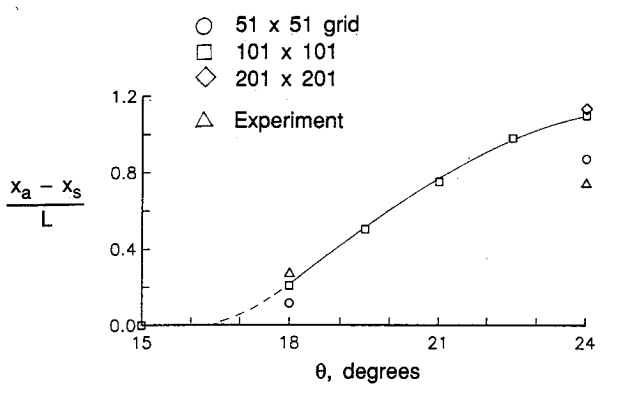

Fig. 6 Effect of wedge angle on extent of separation, CFL3D solutions.

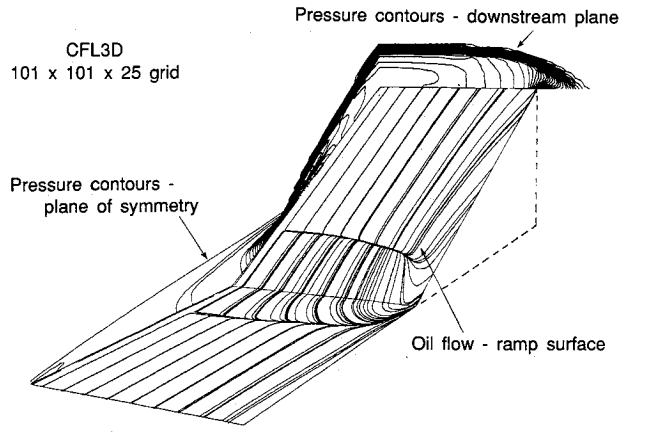

Fig. 8 Three-dimensional solution for 24-deg wedge, CFL3D.

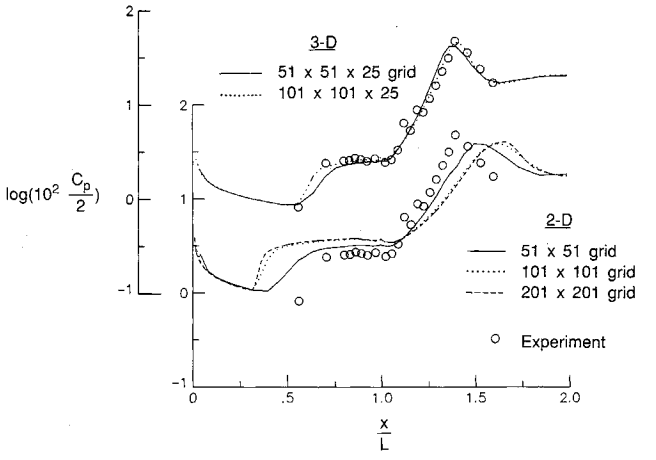

Fig. 9 Comparison of CFL3D computation and experiment for 24-deg wedge.

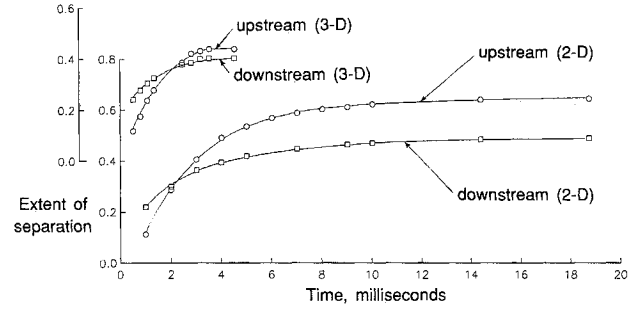

Fig. 10 Time history of separation extent for 214-deg wedge from CFL3D solutions.

steady state has been established in approximately 4 ms, which is in agreement with the experiment.

Summary Comparisons

Figures 11 show a summary comparison of the CFL3D solutions with experimental data for each of the three wedges. The three-dimensional solution in the center plane is shown for the 24-deg wedge, and two-dimensional solutions are shown for both the 15- and 18-deg cases. Excellent agreement of the calculations with experimental data was found for pressure, heat transfer, and skin friction for all three wedge angles.

The present results reconcile several discrepancies between numerical computations and experiment for the 24-deg compression ramp presented in the literature. The original work of Hung and MacCormack[11] in 1976 compared well with the 15- and 18-deg ramp deflections but underpredicted the extent of separation for the 24-deg deflection. This can be attributed to the coarseness of the computational grid in that study since the present investigation indicates that the 24-deg compression ramp requires a much finer grid than that required with the lower angles to attain grid convergence spatially. The more recent work of Ng et al.[13] and Rizzetta and Mach[14] with much finer grids indicate a separation extent that is much larger than experiment for the 24-deg case. These results are consistent with those of the present study in that incorporation of the three-dimensional effect due to spanwise extent is required in order to agree with experiment. Finally, the recent work of Power and Barber[12] indicates less separation than experiment, in contrast to the present results. This smaller predicted extent of separation is believed to be due to a termination of the calculations after the freestream had swept the computational domain four times, which is significantly less than the present calculations indicate are required for the flow to establish a steady state.

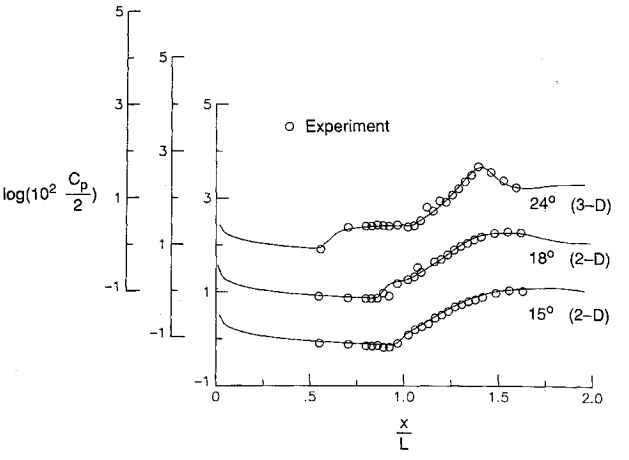

a) Surface pressure

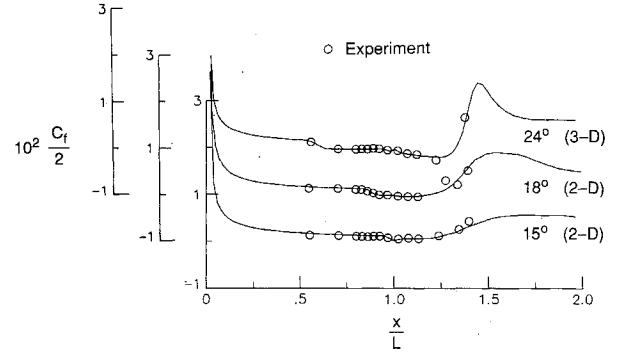

b) Skin friction

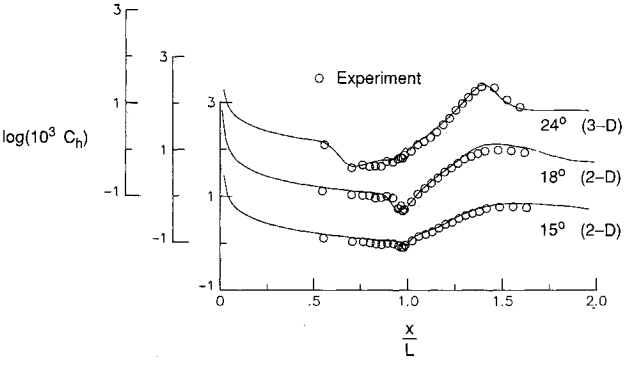

c) Surface heat transfer

Fig. 11 Summary comparison of CFL3D computations and experiment.

Concluding Remarks

A code-validation study has been conducted for four different codes for solving the compressible Navier-Stokes equations. A test case involving high-speed separated flows has been used to compare the results from the codes. Computations for a series of nominally two-dimensional high-speed laminar separated flows were compared with detailed experimental shock-tunnel results. The shock-wave boundary-layer interactions considered were induced by compression ramps with different wedge angles. In general, good agreement was reached between the grid-refined calculations and experiment for the incipient- and small-separation conditions. For the most highly separated flow, three-dimensional calculations,

which included the finite-span effects of the experiment, were required in order to obtain agreement with the data. The finite-span effects were important in determining the extent of separation as well as the time required to establish the steady-flow interaction. The results presented provide a resolution of discrepancies with the experimental data encountered in several recent computational studies.

The present study demonstrated that the four codes are capable of accurately representing both qualitatively and quantitatively the types of complex hypersonic flows with strong viscous-inviscid interactions considered. For sufficiently refined grids, the predictions from the codes were in good agreement with each other and with experimental data considered to be benchmark data for these types of flows. The emphasis of the present study was the grid-refined accuracy of the codes, and, therefore, the study did not address either the issue of the relative efficiency of the codes or the minimum computational requirements to simulate the flows considered.

Acknowledgments

The authors thank M. S. Holden of the Calspan-UB Research Center for fruitful discussions related to the experimental tests and D. P. Rizzetta of the U. S. Air Force Wright Research and Development Center for the interchange of computational results for the compression-ramp study.

References

[1]Rudy, D. H., Kumar, A., Thomas, J. L., Gnoffo, P. A., and Chakravarthy, S. R., "A Comparative Study and Validation of Upwind and Central-Difference Navier-Stokes Codes for High-Speed Flows," *Validation of Computational Fluid Dynamics*, AGARD-CP-437, Vol. 1, Dec. 1988, pp. 37-1–37-15.

[2]Thomas, J. L., Rudy, D. H., Chakravarthy, S. R., and Walters, R. W., "Patched-Grid Computations of High-Speed Inlet Flows," *Advances and Applications in Computational Fluid Dynamics*, ASME FED Vol. 66, Nov.–Dec. 1988, pp. 11–22.

[3]Vatsa, V. N., Thomas, J. L., and Wedan, B. W., "Navier-Stokes Computations of a Prolate Spheroid at Angle of Attack," *Journal of Aircraft*, Vol. 26, No. 11, 1989, pp. 986–993.

[4]Chakravarthy, S. R., Szema, K.-Y., Goldberg, U., Gorski, J. J., and Osher, S., "Application of a New Class of High Accuracy TVD Schemes to the Navier-Stokes Equations," AIAA Paper 85-0165, Jan. 1985.

[5]Gnoffo, P. A., "An Upwind-Biased, Point-Implicit Relaxation Algorithm for Viscous, Compressible Perfect-Gas Flows," NASA TP-2953, Feb. 1990.

[6]Gnoffo, P. A., "Upwind-Biased, Point-Implicit Relaxation Strategies for Viscous Hypersonic Flow," AIAA Paper 89-1972, June 1989.

[7]Kumar, A., "Numerical Simulation of Scramjet Inlet Flow Fields," NASA TP-2517, May 1986.

[8]Kumar, A., "User's Guide for NASCRIN—A Vectorized Code for Calculating Two-Dimensional Supersonic Internal Flow Fields," NASA TM-85708, February 1984.

[9]MacCormack, R. W., "The Effect of Viscosity in Hypervelocity Impact Cratering," AIAA Paper 69-354, April 1969.

[10]Holden, M. S., and Moselle, J. R., "Theoretical and Experimental Studies of the Shock Wave-Boundary Layer Interaction on Compression Surfaces in Hypersonic Flow," ARL 70-0002, Aerospace Research Laboratories, Wright-Patterson AFB, OH, Jan. 1970.

[11]Hung, C. M., and MacCormack, R. W., "Numerical Solutions of Supersonic and Hypersonic Laminar Compression Corner Flows," *AIAA Journal*, Vol. 14, No. 4, 1976, pp. 475–481.

[12]Power, G. D., and Barber, T. J., "Analysis of Complex Hypersonic Flows with Strong Viscous/Inviscid Interaction," *AIAA Journal*, Vol. 26, No. 7, 1988, pp. 832–840.

[13]Ng, W. F., Mitchell, C. R., Ajmani, K., Taylor, A. C., III, and Brock, J. S., "Viscous Analysis of High Speed Flows Using An Upwind Finite Volume Technique," AIAA Paper 89-0001, Jan. 1989.

[14]Rizzetta, D. P., and Mach, K. D., "Comparative Numerical Study of Hypersonic Compression Ramp Flows," AIAA Paper 89-1877, June 1989.

[15]Ota, D. K., Chakravarthy, S. R., and Darling, J. C., "An Equilibrium Air Navier-Stokes Code for Hypersonic Flows," AIAA Paper 88-0419, Jan. 1988.

[16]Korte, J. J., and McRae, D. S., "Explicit Upwind Algorithm for the Parabolized Navier-Stokes Equations," AIAA Paper 88-0716, Jan. 1988.

[17]Lawrence, S. L., Tannehill, J. C., and Chaussee, D. S., "An Upwind Algorithm for the Parabolized Navier-Stokes Equations," AIAA Paper 86-1117, May 1986.

[18]Rudy, D. H., Thomas, J. L., Kumar, A., Gnoffo, P. A., and Chakravarthy, S. R., "A Validation Study of Four Navier-Stokes Codes for High-Speed Flows," AIAA Paper 89-1838, June 1989.